

## Spheromak as a relaxed state with minimum dissipation

B. Dasgupta,<sup>1</sup> M. S. Janaki,<sup>1</sup> R. Bhattacharyya,<sup>1</sup> P. Dasgupta,<sup>2</sup> T. Watanabe,<sup>3</sup> and T. Sato<sup>3</sup>

<sup>1</sup>*Saha Institute of Nuclear Physics, IAF, Bidhannagar, Calcutta 700 064, India*

<sup>2</sup>*Department of Physics, Kalyani University, West Bengal, India*

<sup>3</sup>*Theory and Computer Simulation Center, National Institute of Fusion Science, Toki, Gifu 509-52, Japan*

(Received 12 June 2001; revised manuscript received 16 November 2001; published 25 March 2002)

The principle of minimum dissipation of energy is utilized to obtain the spheromak configuration as a relaxed state. The Euler-Lagrange equation for the minimum dissipative relaxed state is solved in terms of Chandrasekhar-Kendall eigenfunctions analytically generalized in the complex domain. This state is non-force-free and further shows the nonconstancy of the ratio of parallel current to the magnetic field.

DOI: 10.1103/PhysRevE.65.046405

PACS number(s): 52.55.Hc, 52.30.Cv

### I. INTRODUCTION

The spheromak is an axisymmetric compact toroidal magnetic confinement system, where the toroidal field is generated primarily by internal plasma currents. It is characterized by the presence of both toroidal and poloidal fields of nearly equal strength. The analogy of spheromaks can be found in the classical ‘‘Hill’s vortex’’ solutions of fluid dynamics.

The spheromak equilibrium configuration was characterized by Rosenbluth and Bussac [1] as a Taylor relaxed state. Taylor’s relaxation model [2] conjectured that the magnetic field in a plasma relaxes towards a state of minimum energy subject to the constraint of constant magnetic helicity. In a closed system, the minimum-energy equilibrium satisfies the force-free equation  $\nabla \times \mathbf{B} = \lambda \mathbf{B}$  with  $\lambda = \text{const}$ . Many theoretical studies on spheromak equilibria and stability have been undertaken on the basis of this Taylor state predicting relaxed states with constant  $J_{\parallel}/B$  profile and zero pressure gradient. Apart from this relaxation model, the spheromak equilibrium has also been shown to result from the numerical solutions [3] of Grad-Shafranov equation with or without pressure gradient. The formation, sustainment, and decay of spheromaks has also been extensively studied [4,5] through numerical simulation of nonlinear equations of resistive magnetohydrodynamics.

Recently, a number of interesting experimental works [6–11] on spheromaks have revealed that with their compact, robust, and simple structures, the spheromaks have the potential to develop into attractive fusion reactors. Several experimental projects like SSX in Swarthmore, SSPX in LLNL and others have been undertaken to explore this possibility. Earlier investigations (CTX in LANL) have demonstrated good confinement and achieved  $T_e \approx 400$  eV [8,9] and peak electron beta  $> 20\%$  [10,11]. Experimental measurements on spheromak configurations show [12,13] nonconstant  $J_{\parallel}/B$  profiles, which imply a deviation from minimum-energy state. These features of spheromak (e.g., nonzero pressure gradient, nonconstant values of  $J_{\parallel}/B$ , etc.) are studied by solving the Grad-Shafranov equation [14–16] and also through numerical simulation methods.

The theoretical approach to the spheromak has, so far, been largely based on the view that the spheromak is essentially a Taylor state. The Taylor state, being force free, is devoid of pressure gradient and essential confinement fea-

tures. The current interest in spheromak as a potential fusion reactor—which would necessarily confine a high beta plasma—motivates development of an appropriate theory for the spheromak that would predict the observed experimental features such as finite pressure gradient, nonconstant radial profile of  $J_{\parallel}/B$ , etc., at least qualitatively.

A small amount of resistivity, ingrained in any realistic plasma, is essential to allow reconnective processes leading to relaxation. In fact, dissipation, along with nonlinearity, is ubiquitous in systems evolving towards self-organized states and we believe that dissipation plays a decisive role in the self-organization of a system. In a search for the existence of a relaxed state that would support a finite pressure gradient, we invoke the principle of minimum dissipation. This is closely related to the principle of minimum entropy production of irreversible thermodynamics. The rationale behind this principle is as follows. An isolated system with dissipation does not have a true minimum-energy state except for the trivial case of zero field. An absolutely stable relaxed state of the plasma dictated by a minimum-energy principle is, therefore, of little practical interest. On the other hand, a fairly long-lived state can be observed in practice if the rate of dissipation is kept at minimum. A real turbulent plasma with dissipation can indeed ‘‘relax’’ to such a state if small-scale fluctuations stabilize within the resistive time scale. The rate of energy dissipation is sensitive to the higher- $k$  modes in the spectrum of turbulence and if dissipation leads to suppression of large- $k$  modes, the local field distribution becomes nearly stable with minimum dissipation rate. Thus in the relaxation process, small scale fluctuations are stabilized first leading to relatively stable (long-lived) states.

The principle of minimum dissipation, first utilized by Montgomery and Phillips [16], has been applied successfully to show that plasma can relax to a state other than force free and these classes of relaxed states can support a nonzero pressure gradient [17], together with the field reversal for reversed field pinches.

In this work, we propose to identify the observed state of plasma in the actual ‘‘decaying’’ spheromak experiments with precisely this kind of a minimum dissipation state. We derive the spheromak configuration from the equation describing the relaxed state of a magnetized plasma with minimum dissipation so that it can be described as a ‘‘minimum dissipation constant helicity’’ (MDCH) state, rather than a

“minimum energy constant helicity” state. The spheromak when viewed as MDCH state, turns out to be a non-force-free state supporting a significant fraction of perpendicular component of current and is closer to the present day experimental results.

## II. EULER LAGRANGE EQUATION FOR MINIMUM DISSIPATION STATE

The ohmic dissipation rate [16] for a magnetofluid is given by

$$R = \eta \int \mathbf{J}^2 d\tau, \quad (1)$$

where  $\eta$  is the plasma resistivity and the integral is over the entire confinement region. Here  $\eta$  is considered to be independent of space. The magnetic helicity  $K = \int \mathbf{A} \cdot \mathbf{B} d\tau$  is an invariant of motion in ideal magnetohydrodynamics (MHD). If the turbulence is sufficiently low,  $K$  still serves as a constraint [18] as it decays at a slower rate compared to  $R$ . If the energy dissipation rate given by Eq. (1) is minimized by including helicity as a constraint on the minimization through the use of Lagrange’s multiplier  $\bar{\lambda}$ , the following variational equation is obtained:

$$\delta \int (\eta \mathbf{J}^2 + \bar{\lambda} \mathbf{A} \cdot \mathbf{B}) d\tau = 0. \quad (2)$$

On simplification, this leads to

$$\int (\nabla \times \nabla \times \mathbf{J} - \Lambda \mathbf{B}) \cdot \delta \mathbf{A} dV - \oint \left[ \left( \nabla \times \mathbf{J} - \frac{\Lambda}{2} \mathbf{A} \right) \times \delta \mathbf{A} + \mathbf{J} \times \nabla \times \delta \mathbf{A} \right] \cdot d\mathbf{S} = 0,$$

where the last term is a surface integral over the plasma boundary. The surface integrals vanish on considering variations  $\delta \mathbf{A}$  that are zero at the bounding surface. The solution of this variational problem is obtained as

$$\nabla \times \nabla \times \nabla \times \mathbf{B} = \Lambda \mathbf{B}, \quad (3)$$

where  $\Lambda = -\bar{\lambda}/\eta$  is a constant.

## III. SPHEROMAK SOLUTIONS OF $\nabla \times \nabla \times \nabla \times \mathbf{B} = \Lambda \mathbf{B}$

The spheromak solutions of the equation characterizing the relaxed state of a magnetoplasma controlled by the principle of minimum dissipation, can be constructed [17] as a linear combination of the solutions of the force-free equation analytically generalized to the complex domain. Finite beta spheromak equilibria has also been shown [19] to result from the solutions of the static MHD equilibrium equation by a method involving the superposition of eigenfunctions of the force-free equation belonging to real eigenvalues.

A general solution of the force-free equation can be given in terms of the Chandrasekhar and Kendall (CK) eigenfunctions [20] that can be constructed by noting that any mag-

netic field  $\mathbf{B}$ , being a solenoidal field can be decomposed into its toroidal and poloidal components,

$$\mathbf{B} = \mathbf{B}_T + \mathbf{B}_P. \quad (4)$$

The toroidal magnetic field  $\mathbf{B}_T$  and the poloidal magnetic field  $\mathbf{B}_P$  are of the following form:

$$\mathbf{B}_T = -\nabla \times (\mathbf{r}\Psi), \quad \mathbf{B}_P = -\nabla \times \nabla \times (\mathbf{r}\Phi), \quad (5)$$

where  $\mathbf{r}$  is a position vector,  $\Psi$  and  $\Phi$  are any scalar functions of position. In general,  $\Psi$  and  $\Phi$  are distinct and will be related to the toroidal and poloidal flux functions, respectively. It can be shown that if  $\mathbf{B}_0$  satisfies the equation for force-free fields, then

$$\mathbf{B}_0 = -\nabla \times (\mathbf{r}\Psi_0) - \nabla \times \nabla \times (\mathbf{r}\Phi_0), \quad (6)$$

and the following relations must hold:

$$(\nabla^2 + \lambda^2)\Psi_0 = 0, \quad \Phi_0 = \Psi_0/\lambda. \quad (7)$$

In spherical coordinates  $(r, \theta, \phi)$ ,  $\Psi_0$  is obtained as

$$j_m(\lambda r) P_m^n(\cos \theta) e^{in\phi}, \quad (8)$$

where  $j_m(\lambda r)$  is the spherical Bessel function,  $P_m^n(\cos \theta)$  is an associated Legendre function. The classical spheromak equilibrium solution, obtained by Rosenbluth and Bussac [1] is given by  $n=0, m=1$  state together with the boundary conditions  $\mathbf{B}_0 \cdot \mathbf{n} = 0$  at the plasma surface. This yields  $\lambda a = 4.493$ , where  $a$  is the radius. The lines of constant poloidal magnetic field are described by the poloidal flux function  $\chi_0$ , given by

$$\chi_0 = r \sin \theta \frac{\partial \Phi_0}{\partial \theta}. \quad (9)$$

Thus for a force-free state, the toroidal flux function and the poloidal flux function can be obtained from a single scalar function. However, this may not be the most general situation.

The solution of Eq. (3) can be written as a linear combination of the solutions for the force-free equation corresponding to complex eigenvalues

$$\mathbf{B} = \sum_{i=0}^3 \alpha_i \mathbf{B}_i, \quad (10)$$

where  $\alpha_i$  are constants to be fixed by boundary conditions and  $\mathbf{B}_i$  obey the following equations:

$$\nabla \times \mathbf{B}_i = \lambda \omega^i \mathbf{B}_i, \quad (11)$$

where  $\omega$  is the complex cube root of unity. Following Eq. (6),  $\mathbf{B}_i$  can be expressed as

$$\mathbf{B}_i = -\nabla \times \mathbf{r}\Psi_i - \frac{\omega^{2i}}{\lambda} \nabla \times \nabla \times (\mathbf{r}\Psi_i), \quad (12)$$

where  $\Psi_i$  are solutions of

$$(\nabla^2 + \lambda^2 \omega^{2i}) \Psi_i = 0. \quad (13)$$

Following the above, the solution given in Eq. (10) can be expressed as

$$\mathbf{B} = -\nabla \times (\mathbf{r}\Psi) - \nabla \times \nabla \times (\mathbf{r}\Phi), \quad (14)$$

with

$$\Psi = \sum_{i=0}^2 \alpha_i \Psi_i, \quad \Phi = \frac{1}{\lambda} \sum_{i=0}^2 \alpha_i \omega^{2i} \Psi_i. \quad (15)$$

$\Psi_i$  are the generalization in complex domain of the expression given in Eq. (8) and are given by

$$\Psi_i = j_m(\lambda \omega^i r) P_m^n(\cos \theta) e^{in\phi}. \quad (16)$$

The expression for  $\mathbf{B}$  given by Eq. (10) then satisfies Eq. (3) for  $\Lambda = \lambda^3$ . The spheromak solutions of Eq. (3) are given by the  $m=0, n=1$  state as in the earlier case.

The corresponding flux function  $\chi$  is given by

$$\chi(r, \theta) = r \sin \theta \frac{\partial \Phi}{\partial \theta} = -\frac{r}{\lambda} \sum_{i=0}^2 \alpha_i \omega^{2i} j_1(\lambda \omega^i r) \sin^2 \theta. \quad (17)$$

In terms of the poloidal flux function  $\chi$ ,  $\mathbf{B}$  can be written as

$$\mathbf{B} = (\nabla \chi \times \nabla \phi) + r \sin \theta \frac{\partial \Psi}{\partial \theta} \nabla \phi.$$

The different magnetic field components are obtained as

$$\begin{aligned} B_r &= \frac{-2}{\lambda r} \sum_{i=0}^2 \alpha_i \omega^{2i} j_1(\lambda \omega^i r) \cos \theta, \\ B_\theta &= \frac{1}{\lambda r} \sum_{i=0}^2 \alpha_i \omega^{2i} \frac{d}{dr} [r j_1(\lambda \omega^i r)] \sin \theta, \\ B_\phi &= -\sum_{i=0}^2 \alpha_i j_1(\lambda \omega^i r) \sin \theta, \end{aligned} \quad (18)$$

and are shown to lead to spheromak type solutions under appropriate boundary conditions.

### A. Boundary conditions

The boundary conditions are necessary to determine the eigenvalue  $\lambda a$  and for fixing the amplitudes of the non-Taylor part in the solution. Since it is known that the lowest eigenvalue corresponds to states with minimum dissipation, we shall determine the lowest eigenvalue from the boundary conditions,

$$\mathbf{B} \cdot \mathbf{n} = 0, \quad \mathbf{J} \cdot \mathbf{n} = 0 \quad \text{at } r = a, \quad (19)$$

where  $a$  is the boundary of the spheromak. These are the boundary conditions relevant to an insulating boundary at the edge of the spheromak. Also, the condition  $\mathbf{J} \cdot \mathbf{n} = 0$  at  $r = a$  is also equivalent to  $B_\phi = 0$  at  $r = a$  as we are considering the

spherically symmetric solutions with  $n=0$ . This feature is consistent with the classical spheromak solutions obtained in Ref. [1]. The boundary conditions given by Eq. (19) can be realized with three different choices, listed below.

(i) We choose  $\alpha_1, \alpha_2$  to be complex. In order that the fields may be real, this leads to the choice  $\alpha_2 = \alpha_1^*$ , where the asterisk refers to complex conjugate. In this case, the two boundary conditions are utilized to obtain the eigenvalue  $\lambda a$  and also fix the complex ratio partly, say the real or the imaginary part. We are then left with a choice for fixing the other component of the ratio; this amounts to choosing a suitable mixture of the non-force-free part, consistent with the prescribed boundary conditions.

(ii) We can have  $\alpha_i$  to be purely imaginary. In this situation, the boundary conditions determine the eigenvalue  $\lambda a$  and the coefficients for the non-force-free part unambiguously and it also leads to  $\alpha_2 = (\alpha_1)^*$ . The imaginary part of  $\alpha_i$  is given by

$$\text{Im} \left[ \frac{\alpha_1}{\alpha_0} \right] = \frac{B_{0r}}{2 \text{Im}[B_{1r}]}. \quad (20)$$

The lowest eigenvalue for this case is obtained as  $\lambda a = 2.58$ .

(iii) As a third choice, we take  $\alpha_i$  as real. This leads to  $\alpha_1 = \alpha_2$  in order that all fields are real. In this case also the boundary conditions fix the eigenvalue  $\lambda a$  and the amplitude of the non-force-free part completely. We get

$$\begin{aligned} j_1(\lambda a) + 2 \frac{\alpha_1}{\alpha_0} \text{Re}[\omega^2 j_1(\lambda \omega a)] &= 0, \\ j_1(\lambda a) + 2 \frac{\alpha_1}{\alpha_0} \text{Re}[j_1(\lambda \omega a)] &= 0. \end{aligned} \quad (21)$$

The above equations when solved simultaneously lead to the lowest eigenvalue  $\lambda a = 6.09$  and

$$\frac{\alpha_1}{\alpha_0} = - \frac{B_{0r}}{2 \text{Re}[B_{1r}]} \Big|_{r=a}. \quad (22)$$

### B. Location of magnetic axis and $q$ values

The poloidal magnetic field of the spheromak,  $\mathbf{B}_P$  is given by

$$\mathbf{B}_P = \frac{1}{r^2 \sin \theta} \frac{\partial \chi}{\partial \theta} \mathbf{e}_r - \frac{1}{r \sin \theta} \frac{\partial \chi}{\partial r} \mathbf{e}_\theta.$$

The poloidal field has a neutral point at

$$\frac{\partial \chi}{\partial \theta} = 0, \quad \frac{\partial \chi}{\partial r} = 0.$$

Substituting for  $\chi$  from Eq. (17), the magnetic axis of this configuration is described by the circle  $\theta = \pi/2$  and  $r = r_0$ , where  $r_0$  is the solution of

$$\frac{d}{dr} \left( r \sum_{i=0}^2 \alpha_i j_1(\lambda \omega^i r) \right) = 0.$$

The safety factor  $q(\chi)$  has an important role in the stability theory of plasmas and is defined by

$$q(\chi) = \frac{1}{2\pi} \int \frac{B_\phi}{\sin \theta B_\theta} d\theta = -\frac{1}{2\pi} \int \frac{r B_\phi}{\partial \chi / \partial r} d\theta. \quad (23)$$

In the following, we use Eq. (23) in order to obtain the  $q$  values of aspheromak configuration at the magnetic axis and the edge.

### 1. $q$ at the magnetic axis $r=r_0$

At the magnetic axis,  $\partial \chi / \partial r = 0$  as seen from the definition of magnetic axis. So in order to obtain  $q$  value at this point we expand  $\chi$  about the magnetic axis in a Taylor's series [21]

$$\chi = \chi_0 + \frac{(r-r_0)^2}{2} \frac{\partial^2 \chi}{\partial r^2} + \frac{(\theta-\theta_0)^2}{2} \frac{\partial^2 \chi}{\partial \theta^2}, \quad (24)$$

where  $\chi_0$  is the value of  $\chi$  at the magnetic axis and the terms containing first derivatives vanish.

From the above, we can write

$$\frac{d\chi}{dr} = (r-r_0) \frac{\partial^2 \chi}{\partial r^2} \Big|_{r=r_0, \theta=\theta_0},$$

$$(r-r_0) \chi_{rr} = \sqrt{\chi_{rr} \chi_{\theta\theta}} \sqrt{\frac{2(\chi-\chi_0)}{\chi_{\theta\theta}} - (\theta-\theta_0)^2}, \quad (25)$$

where

$$\chi_{rr} = \frac{\partial^2 \chi}{\partial r^2}, \quad \chi_{\theta\theta} = \frac{\partial^2 \chi}{\partial \theta^2}.$$

With these substitutions,  $q_0$  is obtained as

$$q_0 = -\frac{1}{\pi} \frac{r_0 \sum_{i=0}^2 \alpha_i \omega^{2i} j_1(\lambda \omega^i r_0)}{\sqrt{\chi_{rr} \chi_{\theta\theta}}} \times \int_{\pi/2}^{3\pi/2} \frac{\sin \theta}{\sqrt{2(\chi-\chi_0)/\chi_{\theta\theta} - (\theta-\theta_0)^2}} d\theta,$$

$$q_0 = -\frac{1}{\pi} \frac{r_0 \sum_{i=0}^2 \alpha_i \omega^{2i} j_1(\lambda \omega^i r_0)}{\sqrt{\chi_{rr} \chi_{\theta\theta}}} \sin^{-1} \frac{(\theta-\theta_0)}{\sqrt{\frac{2(\chi-\chi_0)}{\chi_{\theta\theta}}}} \Big|_{-1}^1.$$

Finally, the value of  $q$  at the magnetic axis is given by

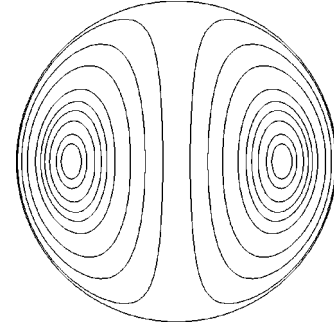


FIG. 1. The spheromak.

$$q_0 = r_0 \frac{\sum_{i=0}^2 \alpha_i j_1(\lambda \omega^i r_0)}{\sqrt{\chi_{rr} \chi_{\theta\theta}}}. \quad (26)$$

The values of  $\alpha_i$  as fixed by the boundary conditions are used to obtain the value of  $q_0$  for different values of  $\lambda a$ .

### 2. $q$ on the last flux surface, i.e., $\chi=0$

The value of  $q$  at the edge denoted by  $q_a$  is obtained by numerically integrating the following:

$$q = \frac{1}{2\pi} \int \frac{B_\phi}{\sin \theta B_\theta} d\theta = \int \frac{B_\phi}{r \sin \theta B_r} dr.$$

Substituting for  $B_\phi, B_r$  from Eqs. (18), we obtain

$$q(r=a) = \frac{\lambda}{4\pi} \int_0^a \frac{\sum_{i=0}^2 \alpha_i j_1(\lambda \omega^i r)}{\cos \theta \sum_{i=0}^2 \alpha_i \omega^{2i} j_1(\lambda \omega^i r)} dr. \quad (27)$$

We note that the last flux surface is given by  $\chi=0$ , and consists of two branches.

(i) On the first branch, which is the semicircle at  $r=a$ ,  $r$  is constant and the contribution to the above integral vanishes.

(ii) On the second branch, which is the diameter of the semicircle passing through the origin  $r=0$ ,  $\cos \theta=0, \pi$ , the above integral can be numerically evaluated for different values of  $\lambda a$  using appropriate boundary conditions.

## IV. RESULTS AND DISCUSSIONS

First, we implement the boundary conditions by choosing the ratio  $\alpha_1/\alpha_0$  as complex. As stated earlier, for a given eigenvalue  $\lambda a$ , the real part of the complex ratio can be uniquely fixed and there is a flexibility in choosing the imaginary part (or vice versa). For the eigenvalue  $\lambda a=4.0$ , the boundary conditions are satisfied with  $\text{Re}[\alpha_1/\alpha_0]=0.02$ ,  $\text{Im}[\alpha_1/\alpha_0]=0.03$ . In this situation, the magnetic axis lies at  $r/a=0.66$ . Most interesting features about the spheromak configuration shown in Fig. 1 are the following: the profile of  $\mu = \mathbf{J} \cdot \mathbf{B} / B^2$ , as plotted in Fig. 2, shows non-constant behavior with peaks lying outside the magnetic axis.

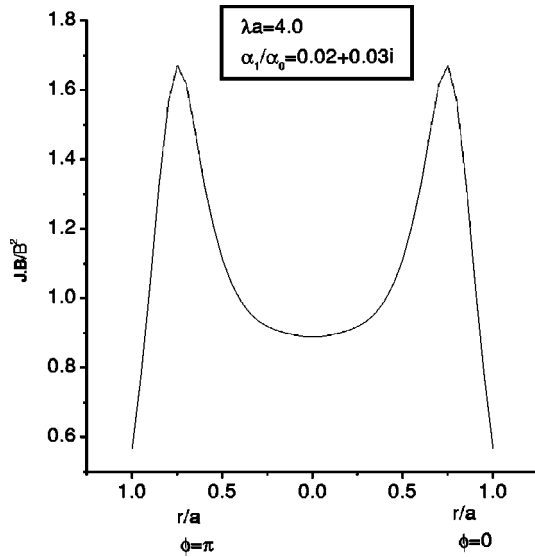


FIG. 2. A plot of  $J_{\parallel}/B$  and against  $r/a$  in the  $z(=r \cos \theta)=0$  midplane for  $\lambda a=4.0$ .

From the figure, it is evident that the characteristics of the profiles obtained from the theory are more realistic and qualitatively closer to the experimentally observed profiles of these quantities [12]. The corresponding profiles of the poloidal ( $B_{\theta}$ ) and toroidal ( $B_{\phi}$ ) magnetic field components in the  $z(=r \cos \theta)=0$  midplane are shown in Fig. 3. The  $q$  values range from 0.58 at the magnetic axis to 0.51 at the edge, showing essentially, as expected, the distinctive low-shear feature of the configuration.

If we take the coefficients  $\alpha_i$ ,  $i=1,2$  as pure imaginary, the boundary conditions lead to  $\alpha_1=(\alpha_2)^*$  and both the eigenvalue and  $\alpha_i$  are determined uniquely. In this case, we obtain the eigenvalue  $\lambda a=2.58$ , and  $\text{Re}[\alpha_1/\alpha_0]=0$ ,  $\text{Im}[\alpha_1/\alpha_0]=0.33$ . The corresponding spheromak configura-

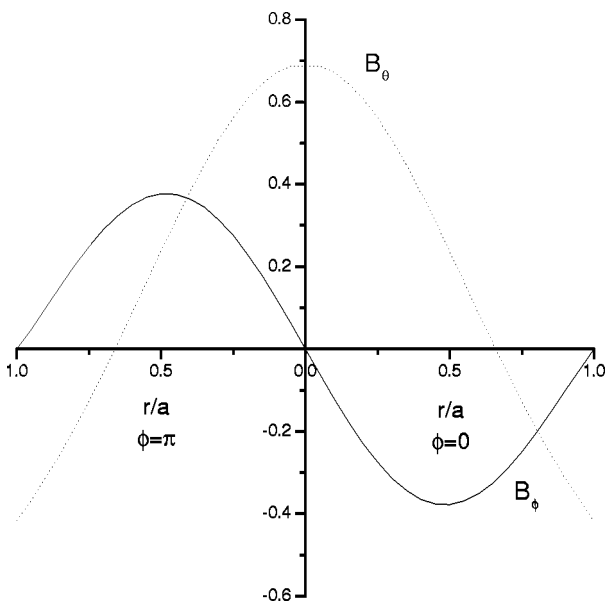


FIG. 3. The profiles of  $B_{\theta}(\dots)$  and  $B_{\phi}(\dots)$  against  $r/a$  in the  $z=0$  midplane for  $\lambda a=4$ .

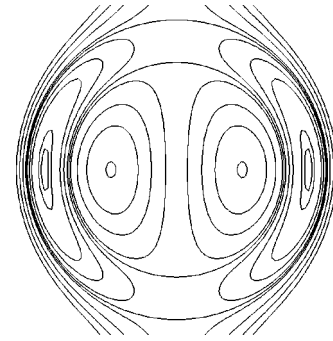


FIG. 4. The double spheromak configuration.

tion is similar to the one obtained in the case of  $\lambda a=4.0$ . Profiles for  $\mu=\mathbf{J}\cdot\mathbf{B}/B^2$  are also similar with more pronounced peaks, i.e., the profiles show a nonconstant behavior of  $\lambda$  profile with peaks closer to the magnetic axis that lies at  $r/a=0.7$ . The values of  $q_0$  and  $q_a$  obtained from Eqs. (26) and (27) are given by 0.143 and 0.142 showing an almost flat  $q$  profile.

A very remarkable feature of the spheromak configuration obtained from this theory is the existence of a double toroidal configuration when  $\alpha_i$  for  $i=1,2$  are chosen real. This type of configuration was earlier described by Morikawa [3] who obtained this from the solutions of a Grad-Shafranov equation by choosing a linearly varying pressure profile with flux function. For real  $\alpha_i$ ,  $i=1,2$  the boundary conditions give the eigenvalue  $\lambda a$  as 6.02, and  $\alpha_1=\alpha_2=-0.012$ . Here we have two magnetic axis locations, one at  $r/a=0.44$  and the other at  $r/a=0.8$ . This gives rise to a double spheromak configuration as shown in Fig. 4. The value of  $q$  at the first magnetic axis is 0.91 and at the edge  $q_a=0.69$ .

A relaxation model based on the principle of minimum rate of energy dissipation is set up leading to an Euler-Lagrange equation that supports non-force-free magnetic fields. The solutions are obtained through an analytic generalization of the CK eigenfunctions to the complex domain. A suitable choice of boundary conditions consistent with experimental observations leads to solutions that represent a spheromak configuration. The boundary conditions fix the eigenvalue  $\lambda a$  and the amplitude of the non-Taylor part of the solution, when the amplitude is completely real or imaginary. However, for complex values of the amplitude, these boundary conditions fix the eigenvalue and allow a free choice of one of the components of the complex amplitude.

The Euler-Lagrange equation describing the minimum dissipation-constant helicity relaxed state is essentially solved in terms of force-free solutions expressed in the form of CK eigenfunctions generalized to the complex domain. However, a final non-force-free state results owing to superposition of the force-free solutions belonging to different eigenvalues. Static MHD equilibria supporting finite pressure profiles can also be formed [19] by summing the orthonormal basis functions of the force-free equation belonging to real eigenvalues. These finite beta spheromak equilibria show departure from a single mode spectrum identified with the Taylor state as pressure increases. The spheromak configuration obtained in this work is shown to result from a

relaxation mechanism based on minimum dissipation rate principle. In analogy with Morse's work [19], the Euler-Lagrange equation obtained by us has both force-free and non-force-free solutions as each of the force-free solutions represented by Eqs. (11) is also a solution of Eq. (3). While the force-free solutions do not give rise to pressure profiles, non-force-free states are capable of supporting a finite beta or flows containing nonzero vorticity. While it is true that superposition almost always leads to non-force-free states, the average beta obtained in the case of non-force-free states depends strongly on the nature of superposition [19]. From this perspective of the nature of pressure or flow profiles, it may be said that the minimum dissipation rate principle provides a means of choosing the solutions to superpose and also has a definite influence on these profiles. Besides, the self-organization mechanism based on the minimum dissipation rate principle automatically leads to the necessity of finding such a superposed solution and is also representative of the physical processes occurring in the magnetized plasma in presence of small but finite resistivity.

The spheromak configuration obtained here is a non-force-free relaxed state unlike Taylor's force-free spheromak and hence supports a perpendicular component of current. Since the magnetic fields given by Eqs. (18) and the associ-

ated current profiles have a nonvanishing  $\nabla \times (\mathbf{J} \times \mathbf{B})$ , the  $\mathbf{J} \times \mathbf{B}$  force tends to be balanced by a tensorial pressure or vortical flows. The plasma configuration considered here corresponds to that of a closed system in the absence of any external drive. Such an isolated system with dissipation relaxes to a fairly long-lived state when small-scale fluctuations stabilize on the resistive dissipation scale. However, an exact representation of equilibrium in terms of flows or pressure through the use of stationary MHD equations may not be valid as in the case of sustained equilibrium in driven systems.

The spheromak solutions obtained here also give rise to nonconstant  $\lambda = \mathbf{J} \cdot \mathbf{B} / B^2$  profiles. Many of the works trying to model spheromak configuration in the framework of Taylor's theory assume an arbitrary variation of  $\lambda$  with the flux function  $\psi$ . We emphasize that this is mathematically inconsistent, as  $\lambda$ , introduced in the theory as a "Lagrange undetermined multiplier" in the variational calculation, is assumed to be a constant. The relaxed states obtained here can support a finite value of beta and hence will be more suitable to describe future spheromak experiments that are supposed to operate at higher beta and hence will exhibit significant pressure profiles that modify the equilibrium magnetic flux functions.

- 
- [1] M. N. Rosenbluth and M. N. Bussac, *Nucl. Phys.* **19**, 489 (1979).
- [2] J. B. Taylor, *Phys. Rev. Lett.* **33**, 1139 (1974).
- [3] T. Yeh and G. K. Morikawa, *Phys. Fluids* **14**, 781 (1971).
- [4] Y. Ono and M. Katsurai, *Nucl. Fusion* **31**, 233 (1991).
- [5] C. R. Sovinec, J. M. Finn, and D. del-Castillo-Negrete, *Phys. Plasmas* **8**, 475 (2001).
- [6] *The Spheromak Path to Fusion Energy*, edited by E. B. Hooper Lawrence, Livermore National Laboratory Report No. UCRL-ID-130429, 1988 (unpublished).
- [7] T. R. Jarboe, *Plasma Phys. Controlled Fusion* **36**, 994 (1994).
- [8] J. C. Fernandez, C. W. Barnes, T. R. Jarboe, I. Henins, H. W. Hoida, P. Klingner, S. O. Knox, G. J. Marklin, and B. L. Wright, *Nucl. Fusion* **28**, 1555 (1988).
- [9] T. R. Jarboe, F. J. Wysocki, J. C. Fernandez, I. Henins, and G. J. Marklin, *Phys. Fluids B* **2**, 1342 (1990).
- [10] F. J. Wysocki, J. C. Fernandez, I. Henins, T. R. Jarboe, and G. J. Marklin, *Phys. Rev. Lett.* **65**, 40 (1990).
- [11] F. J. Wysocki, J. C. Fernandez, I. Henins, T. R. Jarboe, and G. J. Marklin, *Phys. Rev. Lett.* **61**, 2457 (1988).
- [12] G. W. Hart, C. Chin-Fatt, A. W. DeSilva, G. C. Goldenbaum, R. Hess, and R. S. Shaw, *Phys. Rev. Lett.* **51**, 1558 (1983).
- [13] S. O. Knox, C. W. Barnes, G. J. Marklin, T. R. Jarboe, I. Henins, H. W. Hoida, and B. L. Wright, *Phys. Rev. Lett.* **56**, 842 (1986).
- [14] C. G. R. Geddes, T. W. Kornack, and M. R. Brown, *Phys. Plasmas* **5**, 1027 (1998).
- [15] D. A. Kitson and P. K. Browning, *Plasma Phys. Controlled Fusion* **32**, 1265 (1990).
- [16] D. Montgomery and L. Phillips, *Phys. Rev. A* **38**, 2953 (1988).
- [17] B. Dasgupta, P. Dasgupta, M. S. Janaki, T. Watanabe, and T. Sato, *Phys. Rev. Lett.* **81**, 3144 (1998).
- [18] R. Bhattacharyya, M. S. Janaki, and B. Dasgupta, *Phys. Plasmas* **7**, 4801 (2000).
- [19] E. C. Morse, *Phys. Plasmas* **5**, 1354 (1998).
- [20] S. Chandrasekhar and P. C. Kendall, *Astrophys. J.* **126**, 457 (1991).
- [21] S. Kaneko, A. Takimoto, M. Taguchi, and T. Miyazaki, *J. Phys. Soc. Jpn.* **53**, 201 (1984).